Shape dynamics of interfacial front in rotating cylinders

Gerald H. Ristow[1] and Masami Nakagawa[2]

[1]*Fachbereich Physik, Philipps-Universität, Renthof 6, 35032 Marburg, Germany*
[2]*Division of Engineering, Colorado School of Mines, Golden, Colorado 80401*

The evolution of the interface propagation in a slowly rotating half-filled horizontal cylinder is studied using magnetic resonance imaging. Initially, the cylinder contains two axially segregated bands of small and large particles with a sharp interface. The process of the formation of the radial core is clearly captured, and the shape and the velocity of the propagating front are calculated by assuming a one-dimensional diffusion process along the rotation axis of the cylinder and a separation of time scales associated with segregation in the radial and axial directions. We found that the interfacial dynamics are best described when a concentration-dependent diffusion process is assumed. [S1063-651X(99)06002-X]

I. INTRODUCTION

When granular materials are put in a horizontal rotating cylinder, most particles undergo a solid body rotation except for a thin layer of particles flowing near the free surface. With increasing rotation rate, particles first exhibit intermittent avalanches, then continuous flow near the surface, and finally a ring structure due to centrifugal force [1]. In industrial applications, rotating cylinders are primarily used for mixing different components [2]. But it is well known that particles of different size or density show radial segregation on small time scales and axial segregation on large time scales which compete against the mixing process [2–9].

One of the ways to investigate the three-dimensional particle motion is to stop the rotating cylinder and take samples from different locations [10]. However, this inevitably involves a partial destruction of the internal structure which might provide vital information. Another shortcoming of this approach is that it is time consuming to obtain global information about the particle motion. Recently, noninvasive magnetic resonance imaging (MRI) has been used to interrogate the internal structures of evolving granular assemblies [11]. Since the current MRI flow measurement is designed for a steady flow of particles and recording a single image can take several minutes, the cylinder is also stopped to capture a series of static images of the propagating front starting with the same set of initial conditions. Nakagawa *et al.* [11] first applied MRI to study the dynamics of granular flow in a rotating cylinder and recorded velocity and density profiles along and perpendicular to the flowing layer of particles. Using a spin-tagging sequence, the flow and diffusion in a vertically shaken container of poppy seeds was recently measured and convection rolls found [12]. Most recently, the shape of the radially and axially segregated core was also investigated by MRI [9,13].

Not much is known yet about how this radially segregated core evolves. In the common segregation experiments, one starts with a well mixed initial state containing small and large particles. The formation of a radial core of small particles which extends over the whole length of the cylinder is already visible after a few rotations [4]. This radial core may become unstable forming band patterns, which is called *axial segregation*. This process was best demonstrated by Hill *et al.* [9] using MRI. The final number of bands, their positions, and widths varied from experiment to experiment but Nakagawa [5] found the three-band configuration to be stable after an extended number of rotations. These bands may not be pure and a radial core might still be present, whereas Chicharro *et al.* [7] rotated two sizes of Ottawa sand for two weeks at 45 rpm and found a final state of two *pure* bands each filling approximately half of the cylinder, i.e., *no* radial core was found. Recently, experimental evidences were given for two new mechanisms of axial segregation, namely *traveling waves* [8] and *avalanche mediated transport* [14], which were only observed when nonspherical particles were used.

Since the dynamics of the axial segregation process depends on the homogeneity of the initial mixture, it is desirable to start with a better defined initial packing. We propose to start with a fully axially segregated state of a binary particle mixture and use MRI to investigate the three-dimensional segregation front which is initially seen as a sharp flat interface. We study the propagation velocities and compare them with results obtained from a simple diffusive process where a *concentration-dependent* diffusion coefficient is used. The shape of the segregation front can be calculated approximately analytically when a separation of time scales for the segregation in the radial direction and the diffusion in the axial direction is assumed.

II. EXPERIMENTAL SETUP AND STUDIES

The initial state was prepared in such a way that the left half of the cylinder contained only large particles having a diameter of 4 mm and the right half contained only small particles having a diameter of 1 mm. It is similar to the one used in [15] and is sketched in Fig. 1 where the larger particles are shown in gray. A 50-50 mixture by volume was used and the total volume was chosen to give a roughly half-filled cylinder.

Axial migration of the core of small particles is a three-dimensional process and its dynamics should be monitored by a noninvasive method. The very strength of MRI among other existing noninvasive techniques lies in its ability of
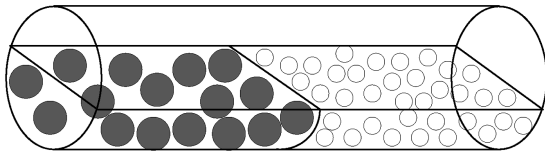
FIG. 1. A simplified sketch of the initial configuration: large particles are all in the left half of the cylinder and shown in gray. This corresponds to the first side view image in Fig. 2.

measuring dynamic flow properties such as velocities and velocity fluctuations. Measurement of true concentration still remains a challenging problem because in granular flows concentration and particle agitation, characterized by the granular temperature, are strongly coupled, which is predicted by kinetic theories. It is not trivial to separate causes for the lesser concentration signals. Less challenging but equally important is MRI's ability to probe a dense static granular system. In fact, the denser the system of interest is, the higher the quality of the images become. Since the MRI technique used is best suited for flows in a steady state, the cylinder was stopped when the images were taken.

Our MRI imager/spectrometer (Nalorac Cryogenics Corp) has a 1.9 tesla superconducting magnet (Oxford) with a bore diameter of 31 cm. The useful space inside the bore is a sphere of diameter of about 8 cm after the insertion of the gradient coils and the rf probe. The acrylic cylinder with 10 cm and 7 cm in its length and diameter, respectively, was rotated at a constant rate of 11.4 rpm by a dc servo motor (12FG) and a controller (VXA-48-8-8) made by PMI inside the imaging apparatus. The material properties, the drum geometry, and its rotation speed were chosen such that the drum was operating in the beginning of the continuous flow regime. Images were taken after 0, 15, 30, 45, 60, 75, 90, and 600 s of rotation. The particles used were spherical pharmaceutical pills of 1 and 4 mm diameter which contain a liquid core of vitamin oil. Louge *et al.* [16] conducted a detailed binary impact experiment using these particles and estimated the normal coefficient of restitution to be about 0.9. In the perpendicular direction, however, they have found that these liquid-filled particles exhibit rolling contacts with negligible compliance.

The cylinder was put into the magnet for recording three-dimensional intensity signals ($64 \times 64 \times 64$ points) which took around 40 min each. Due to the limitations in the spatial resolution, the smaller particles cannot be resolved individually and appear as light gray in the images. Since the larger particles contain more liquid, they give a higher signal and show up in black or dark gray in the images. Despite the fact that our images are three-dimensional, we have decided to illustrate the dynamics of the conical shape of the migrating front by showing two different cross-sectional views in Fig. 2, namely the side views on the left and the top views on the right. Initially (0 sec), the large and small particles were packed in the left and right half of the cylinder, respectively, and the heaping of the large particles at the left end in the top left image is due to an actual uneven initial packing. This quickly disappeared and was flattened to the same level as in other parts of the cylinder once the cylinder was in motion.

The side views were obtained by superimposing the 16 vertical planes in the central region of the cylinder and tak-
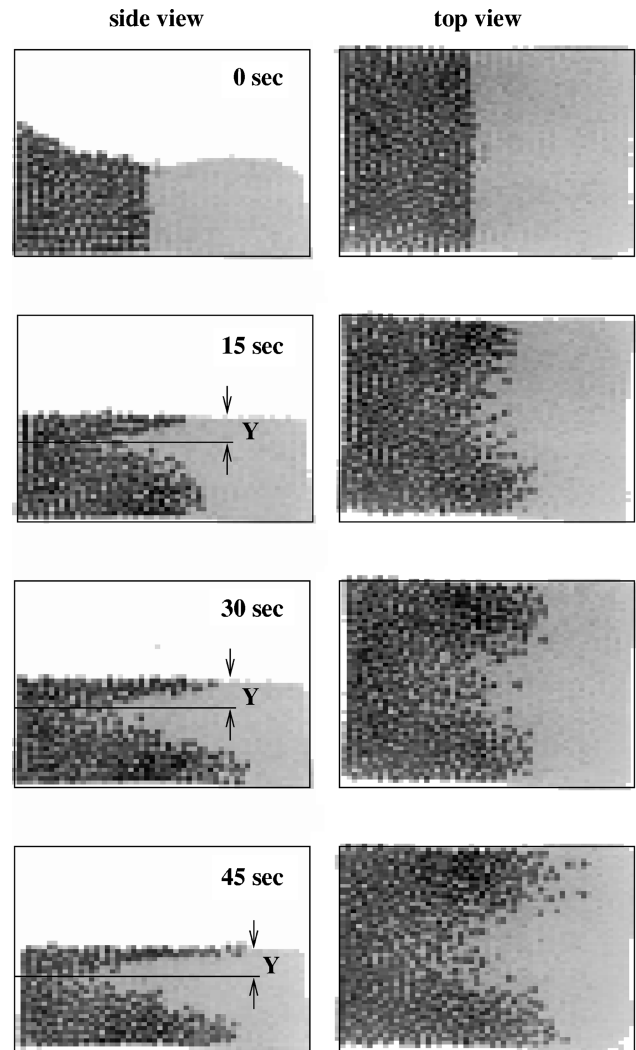

FIG. 2. Cross sectional views of the interface propagation for a mixture of 1- and 4-mm vitamin pills in a half-filled rotating cylinder. The small particles cannot be resolved individually and the region they occupy is shown in light gray.

ing the highest intensity value of all planes. This averaging increased the contrast and we verified that the shape of the front did not change significantly within these planes. For the top view, 12 planes in the lower half of the cylinder were superimposed. By this procedure, we can clearly identify the regions containing large particles without losing spatial information. The time evolution in Fig. 2 shows that the cascading layer is almost entirely composed of large particles whereas the small particles can *sink into* the surface layer more easily and consequently their concentration in the layer will decrease. The distance of the tip of the migrating front of small particles and the free surface, denoted by Y in Fig. 2, remains more or less constant. This indicates that the small particles in the cascading layer are responsible for the front advancement. Immediately after the cylinder starts to rotate, there is a mixture of large and small particles flowing in the cascading layer developed at the interface. Due to the percolation mechanism, the smaller particles travel under the free surface and move in the axial direction driven by the concentration gradient. The smaller particles advance more easily into the region occupied by larger particles since there are
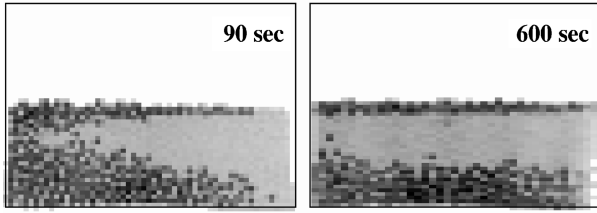
FIG. 3. Side view of the segregation front for later times at 90 s (left) and at 600 s (right) after start of rotation.

more voids in the cascading region for the small particles to move into. We also observed that the larger particles traveling on the surface always reached the other end of the cylinder before the smaller particles did. Eventually, this leads to an extended radially segregated core, shown in Fig. 3 and also observed in other experiments [9].

III. RADIAL CORE DEVELOPMENT

Assuming random particle motion in the axial direction (z axis), one component systems could be well described by a diffusion process according to Fick's second law [10,17]. The interface of a two-component system can also be studied in this fashion and the diffusion equation reads

$$\frac{\partial C(z,t)}{\partial t} = \frac{\partial}{\partial z}\left(D\frac{\partial C(z,t)}{\partial z}\right), \quad (1)$$

where $C(z,t)$ and D denote the relative concentration by volume of the smaller particles and the corresponding diffusion coefficient, respectively. The initial conditions for a cylinder with length L are

$$C(z,0) = \begin{cases} 0, & -\frac{L}{2} \leq z < 0 \\ 1, & 0 < z \leq \frac{L}{2}, \end{cases}$$

whereas the boundary conditions read

$$\frac{\partial C}{\partial z}\bigg|_{z=-L/2} = \frac{\partial C}{\partial z}\bigg|_{z=L/2} = 0,$$

which states that there is zero axial flux at the boundaries due to the end caps.

For a constant diffusion coefficient, Eq. (1) can be solved analytically for the specified initial and boundary conditions and the solution reads

$$C(z,t) = \frac{1}{2} + \frac{2}{\pi}\sum_{k=1}^{\infty}\frac{1}{2k-1}\exp\left\{-\frac{(2k-1)^2\pi^2Dt}{L^2}\right\}$$

$$\times \sin\left\{\frac{(2k-1)\pi z}{L}\right\}. \quad (2)$$

Hogg *et al.* [10] solved a similar diffusion problem for a single component system by replacing the time derivative with the derivative with respect to the number of rotations, thus assuming that the dynamic effects on the diffusion process were not significant within the range of the rotation
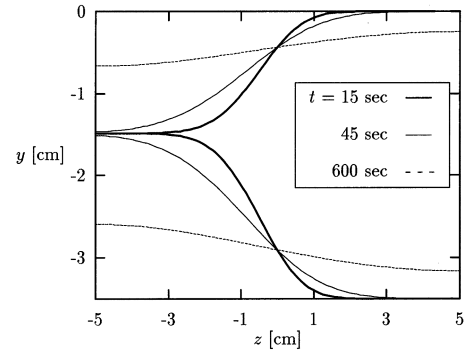

FIG. 4. Theoretical prediction of the interface shape for three different times after the start of rotation using the same constant diffusion coefficient $D = 0.02$ cm^2/s.

rates studied. Nakagawa *et al.* [15] investigated a mixing process of 50-50 mixtures of liquid-filled pharmaceutical pills of different sizes. After different numbers of revolutions they inserted 12 dividers along the rotational axis and measured the fraction of small particles in each of the 13 segments. They obtained one-dimensional concentration profiles similar to the theoretical prediction given by Eq. (2). However, for longer rotation times, their profiles showed a slight asymmetry with respect to the position of the initial front. It should be kept in mind, however, that the final configuration in both our MRI study and Ref. [15] was a radial segregated core of small particles and not a mixture as in Refs. [10,17].

It was found experimentally [2,6] and numerically [18] that a nearly complete radial segregation can be achieved after only a few rotations. In the above, successive MRI pictures were separated by 15 s, which corresponds to roughly three full rotations, and each particle had a chance to participate in approximately six avalanches. In order to calculate analytically the exact shape of the interface of small particles migrating into the region initially occupied by large particles, it is assumed that the concentration change in each section is slow enough that the fully radially segregated core is already completely developed. This approximation states a direct relationship between concentration $C(z,t)$ and width and position of the region occupied by small particles which will be given now.

For a half-filled cylinder, the center of mass of the core of small particles lies $4R/3\pi$ below the free surface. For lower concentrations, we assume that all small particles occupy a region in the shape of a half circle, again centered at the same point as the full half circle. The radius r of this half circle is related to the concentration and the cylinder radius by

$$C = \frac{r^2}{R^2} \Rightarrow r = R\sqrt{C}.$$

The analytically obtained interfacial shape dynamics of the region occupied by small particles is shown in Fig. 4 for three different times after the start of rotation. From the cross-sectional views of Fig. 2, we estimated that the front of small particles reached the left cylinder boundary around $t = 45$ s, which gave a value of $D = 0.02$ cm^2/s for the diffusion coefficient in Eq. (1). Mixing experiments using 6.4 mm lucite beads gave diffusion coefficients around 0.1 cm^2/s
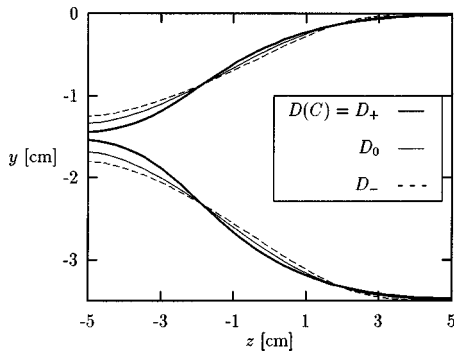
FIG. 5. Theoretical prediction of the interface shape at $t=90$ s for three different concentration dependencies of the diffusion coefficient D.

FIG. 6. Propagation of large particles along rotation axis, comparison of experimental data ($\bullet$) and from the diffusion equation using a constant ($\cdots$) or a concentration-dependent (—) diffusion coefficient D.

and the higher value is due to the larger particle diameter [17]. All shapes agree well with the MRI data considering the level of approximations made and the dashed line for $t=600$ s predicts an already nearly fully radially segregated core of small particles which corresponds well to the right picture of Fig. 3. In order to derive an improved model, however, we need to know the exact shape of the region occupied by small particles and the exact position of the center of mass of this region.

The proposed model with a constant diffusion coefficient D in Eq. (1) always leads to symmetric concentration profiles, which can be seen from Eq. (2). However, the experimental data presented in Ref. [15] indicate that even though this is a good approximation for small numbers of rotations, clear deviations from symmetric profiles are detected for large numbers of rotations. Since particle concentrations vary in space and time and might have different particle packings due to the radial segregation process, the mobility of the particles is also affected. The proposed model enables us to test the effects of a *concentration dependent* diffusion coefficient on the particle motion, especially the shape dynamics. We will investigate two linear dependencies of the form

$$D_{\pm}(C)=D_0 \pm D_0(C-0.5) \qquad (3)$$

which fulfill

$$\langle D \rangle \equiv \int_0^1 D_{\pm}(C)dC = D_0$$

and solve Eq. (1) numerically by using a standard finite-difference procedure.

This linear concentration dependence has a significant effect on the shape dynamics which is shown in Fig. 5 by comparing both laws with the shape given by a constant diffusion coefficient at $t=90$ s. The effect is most pronounced in the left part of the cylinder, i.e., in the region the small particles propagate into. When D increases (decreases) with small particle concentration C, the diameter of the segregated core close to the left cylinder wall is larger (smaller). Unfortunately, we are not able to judge which of the investigated three concentration dependencies of D gives the best agreement with the experimental data. The spatial resolution is not high enough to reconstruct the full shape which would be necessary in order to distinguish a dependence of the form
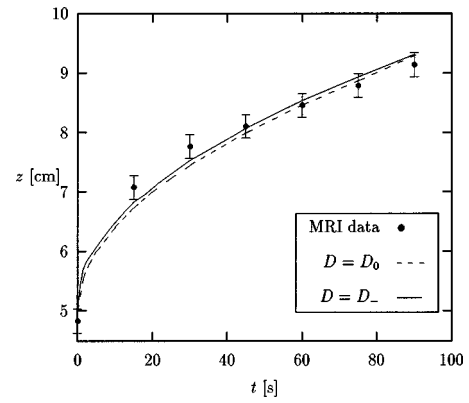
$D_{\pm}(C)$ from a constant diffusion coefficient with a larger (for D_-) or smaller (for D_+) value. However, we will present in the next section a more suitable method to do so.

Since the larger particles give a higher MRI signal, the propagation of these particles into the region initially filled with small particles can be studied by recording intensity values that correspond to large particles. These values were extracted from the side views of Figs. 2 and 3 and are shown in Fig. 6 as filled circles with corresponding error bars. Also shown as a dashed line is the theoretical curve according to Eq. (2) using the same constant diffusion coefficient of $D=0.02$ cm^2/s as in Fig. 4. The data show that the front advancement is underestimated when a constant diffusion coefficient is used. The particle dynamics are very different for particles in the fluidized surface layer and for particles following the solid body rotation. The fluidized surface layer has a thickness of a few large particles for the range of rotation speeds used here. For a low concentration of small particles, these can be trapped in a region well below this layer and they will show a low mobility relative to one another due to percolation. For higher concentrations, the segregated core is large enough so that some of the small particles in the core are mixed with the large particles in the fluidized surface layer. Therefore, not all small particles can remain in the segregated core but some will be recirculated in the flowing layer. The mobility of particles in this layer is much higher than for particles in the segregated core which makes us believe that the diffusion coefficient is concentration dependent.

The exact functional dependence can only be inferred from a detailed understanding of the microscopic particle motion of the two species, e.g., by looking at the asymmetry of the concentration profile or by calculating the diffusion coefficient microscopically. Unfortunately, neither the experimental nor the numerical results available are accurate and detailed enough to address this question fully. However, it is already very instructive to consider the two linear dependencies proposed in Eq. (3) and we show in Fig. 6 as a solid line the numerical result for $D(C)=D_-(C)$. The result for $D(C)=D_+(C)$ will lie between the solid and dashed lines and in either case we get a better agreement with the experimental result as compared to the case in which a constant diffusion coefficient $D(C)=D_0$ is used.

IV. CONCLUSIONS

Using MRI measurements, we investigated the shape dynamics and interface propagation in a slowly rotating half-filled horizontal cylinder. By assuming that the radial segregation and the axial migration process occur on different time scales, we showed that the propagating front can be well described by a one-dimensional diffusion process. The experimentally observed concentration profiles are slightly asymmetrical [15], however this can be understood by using a concentration-dependent diffusion coefficient. We demonstrated the effect when a linear dependence of the diffusion coefficient on the particle concentration is used in the analytic description. In this case, we found a better agreement with the experimental results as compared to the case when the diffusion coefficient is constant. This implies that the shape dynamics of the interface propagation can be described more accurately when a concentration-dependent diffusion coefficient is considered. However, in order to determine the correct concentration dependence of the diffusion coefficient, one must compare the shape of the whole concentration profile or one has to calculate the diffusion coefficient microscopically from the particle movements.

[1] J. Rajchenbach, Phys. Rev. Lett. **65**, 2221 (1990).

[2] J. Bridgewater, Powder Technol. **15**, 215 (1976).

[3] Y. Oyama, Bull. Inst. Phys. Chem. Res. Jpn. Rep. **18**, 600 (1939).

[4] M. B. Donald and B. Roseman, Br. Chem. Eng. **7**, 749 (1962).

[5] M. Nakagawa, Chem. Eng. Sci. **49**, 2544 (1994).

[6] E. Clément, J. Rajchenbach, and J. Duran, Europhys. Lett. **30**, 7 (1995).

[7] R. Chicharro, R. Peralta-Fabi, and R. M. Velasco, in *Powders & Grains 97*, edited by R. P. Behringer and J. T. Jenkins (Balkema, Rotterdam, 1997), p. 479.

[8] K. Choo, T. C. A. Molteno, and S. W. Morris, Phys. Rev. Lett. **79**, 2975 (1997).

[9] K. M. Hill, A. Caprihan, and J. Kakalios, Phys. Rev. Lett. **78**, 50 (1997).

[10] R. Hogg, D. S. Cahn, T. W. Healy, and D. W. Fuerstenau, Chem. Eng. Sci. **21**, 1025 (1966).

[11] M. Nakagawa, S. Altobelli, A. Caprihan, E. Fukushima, and E.-K. Jeong, Exp. Fluids **16**, 54 (1993).

[12] E. E. Ehrichs, H. M. Jaeger, G. S. Karczmar, J. B. Knight, V. Y. Kuperman, and S. Nagel, Science **267**, 1632 (1995).

[13] M. Nakagawa, S. A. Altobelli, A. Caprihan, and E. Fukushima, Chem. Eng. Sci. **52**, 4423 (1997).

[14] V. Frette and J. Stavans, Phys. Rev. E **56**, 6981 (1997).

[15] M. Nakagawa, J. L. Moss, K. Nishimura, and T. Ozeki, in *Powders & Grains 97*, edited by R. P. Behringer and J. T. Jenkins (Balkema, Rotterdam, 1997), p. 495.

[16] M. Y. Louge, C. Tuozzolo, and A. Lorenz, Phys. Fluids **9**, 3670 (1997).

[17] D. S. Cahn and D. W. Fuerstenau, Powder Technol. **1**, 174 (1967).

[18] C. M. Dury and G. H. Ristow, J. Phys. I **7**, 737 (1997).